Electromagnetic Productions of $K\Lambda$ and $K\Sigma$ on the Nucleons

T. Mart

Departemen Fisika, FMIPA, Universitas Indonesia, Depok, 16424, Indonesia

Abstract. We briefly review the progress and problems in the electromagnetic production of $K\Lambda$ on the nucleon. The problem of the data discrepancy in this channel as well as the corresponding physics consequence are highlighted. We also discuss the effect of the new beam-recoil polarization data C_x and C_z on our analysis. For this purpose we use the isobar model Kaon-Maid and a recent multipoles model that can describe recent experimental data. We also present a new multipoles model for the $K\Sigma$ channels to complete our analysis.

Keywords: Kaon photoproduction, multipoles, isospin symmetry
PACS: 13.60.Le, 25.20.Lj, 14.20.Gk

1. INTRODUCTION

One of the most important goals of nuclear and particle physics is a unified understanding of the baryon-baryon interaction. However, unlike in the case of the nucleon-nucleon interactions, our knowledge on the hyperon-nucleon interactions is far from complete. The lack of hyperon beam or target becomes the main reason of this difficulty. Thus, one needs indirect reactions to study this strange particles. On the other hand, the strange quark in this particle generates another degree of freedom and, therefore, gives additional information not available from the nucleon-nucleon scattering processes. As a consequence, investigations of the strange particles remain an interesting research topic nowadays. This is also supported by the fact that hypernuclear studies relies heavily on the available information on the hyperon-nucleon interactions. To this end, the associated production of strange particles is very helpful, both as a source of information on the hyperon-nucleon interaction and as the elementary operator that describes the process at the elementary level. The electromagnetic production of kaon on the nucleon is one of the commonly used reactions for this purpose. Both virtual and real photons can be used. However, since the real photon is theoretically much simpler than the virtual one, we will limit the following discussion to the photoproduction process.

2. ELECTROMAGNETIC PRODUCTIONS OF $K\Lambda$

In what follows, we shall consider two phenomenological models based on the Feynman and multipoles techniques, i.e., the Kaon-Maid model [1, 2] and the recent multipole approach given in Ref. [3]. In the former, tree-level Feynman diagrams have been used to reproduce all available $K^+\Lambda$, $K^+\Sigma^0$ and $K^0\Sigma^+$ photoproduction observables. The background terms contain the standard *s*-, *u*-, and *t*-channel along with a contact

term, which is required to restore gauge invariance after hadronic form factors had been introduced [4]. Furthermore, four nucleon resonances, the $S_{11}(1650)$, $P_{11}(1710)$, $P_{13}(1720)$, and the "missing resonance" $D_{13}(1895)$ have been also included in this model. For $K\Sigma$ production further contributions from the $S_{31}(1900)$ and $P_{31}(1910)$ Δ resonances were added. Note that, Kaon-Maid was fitted to old and previous version of SAPHIR data [5]. An interactive version of this model is available through internet [6].

The multipole model utilizes the same background terms, whereas the resonance parts are assumed to have the Breit-Wigner form [7]

$$A^R_{\ell\pm}(W) = \bar{A}^R_{\ell\pm} c_{KY} \frac{f_{\gamma R}(W)\Gamma_{\rm tot}(W) M_R\, f_{KR}(W)}{M_R^2 - W^2 - iM_R\Gamma_{\rm tot}(W)} e^{i\phi}, \tag{1}$$

where W the total c.m. energy, c_{KY} the isospin factor, f_{KR} the conventional Breit-Wigner factor describing the decay of a resonance R with a total width $\Gamma_{\rm tot}(W)$ and physical mass M_R, $f_{\gamma R}$ the γNR vertex factor, and ϕ the phase angle. The model was fitted to the combinations of the recent SAPHIR [8], CLAS [9], and LEPS [10, 11] data. In spite of their unprecedented high qualities, these new data sets, however, reveal a lack of consistency at the forward and backward kaon angles. This problem hinders the reliable extraction of the resonance parameters, which could lead to different conclusions on the extracted "missing resonances".

2.1. Differences between CLAS and SAPHIR Data

2.1.1. Statistical Differences

Reference [12] has studied the statistical properties of both CLAS and SAPHIR data in a great detail by using four different isobar models. In general it is found that, compared to the other three models, the Kaon-Maid model provides a better description of the presently existing data. Nevertheless, the agreement with the SAPHIR data is more remarkable than with other data, which is indicated by the fact that the SAPHIR data are scattered closer to $R_i = 0$ compared to the CLAS ones (see Fig. 1), where R_i is the relative deviation of each data point, defined by

$$R_i = \frac{\sigma_i^{\rm exp} - \sigma^{\rm th}(E_i, \theta_i)}{\Delta\sigma_i^{\rm stat}}\ . \tag{2}$$

Interestingly, if we analyze this agreement more closely by using the statistical parameter z_1, then a different phenomenon appears. The parameter is defined as

$$z_1 = \sqrt{N-1}\frac{\langle R\rangle}{\sqrt{\langle(\Delta R)^2\rangle}}, \tag{3}$$

where N is the number of data points and $\langle(\Delta R)^2\rangle = \langle R^2\rangle - \langle R\rangle^2$ indicates the square of the variance of the normal distribution of R_i. Provided that the data are randomly scattered around the theoretical values with this variance, the hypothesis that the true

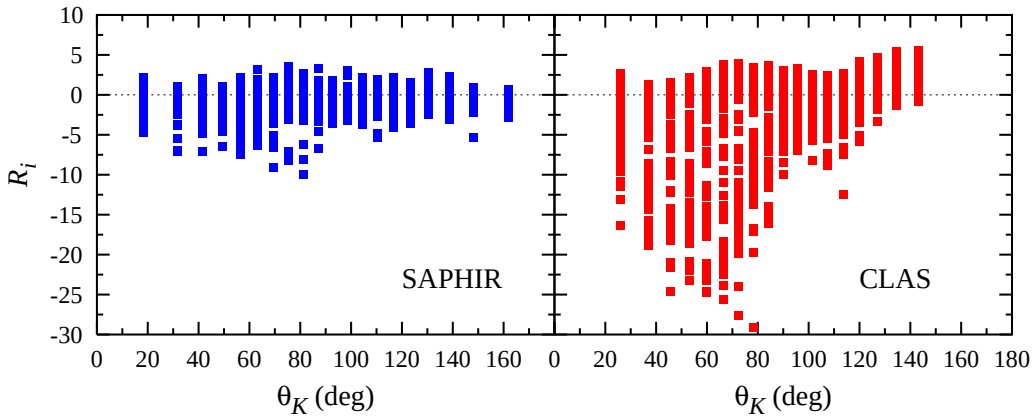

FIGURE 1. Deviations of the predictions of the Kaon-Maid model from the SAPHIR and CLAS experimental data points as a function of the kaon c.m. angle. Note that R_i is defined in Eq. (2).

value of the mean $\langle R \rangle$ equals zero (the null hypothesis) can be rejected with a confidence level of α if $|z_1| > z_{\alpha/2}$, where the critical value $z_{\alpha/2}$ = 1.96 and 2.58 for the confidence level of 5% and 1%, respectively [13].

As shown in Ref. [12], the use of SAPHIR data in Kaon-Maid model yields $|z_1| = 11.7$, whereas the use of CLAS data in the same model results in $|z_1| = 1.41$. Focusing only on the forward-direction data does not change this result. This leads to the conclusion that if we reject the null hypothesis, then there is a large probability that we are wrong. In other words, the Kaon-Maid model is more consistent with the CLAS data.

Recent analyses have also indicated that there could be a global scaling factor between the CLAS and SAPHIR data. To determine this factor, Ref. [12] defined the quantity s through

$$\chi_0^2 \;=\; \sum_{i=1}^{N} \left(\frac{s\sigma_i^{\rm exp} - \sigma^{\rm th}(E_i,\theta_i)}{\Delta\sigma_i^{\rm stat}} \right)^2 , \qquad (4)$$

and minimized the χ_0^2 by using the SAPHIR data, where $\sigma^{\rm th}$ is obtained from the specific isobar model that had been previously fitted to the CLAS data. For the full data set it is found that $s = 1.13$ and for the forward data set the best fit yields $s = 1.15$ [12]. These findings indicate that an increase of the SAPHIR data by a factor of 13% – 15% would improve the agreement between the two data sets. These values are, however, smaller than the previously suggested scaling factor of $\sim 4/3$ [9].

2.1.2. The Physics Consequences

The problem of the lack of mutual consistency between the SAPHIR and CLAS data has certainly some physics consequences. The use of SAPHIR and CLAS data, individually or simultaneously, leads to quite different resonance parameters which,

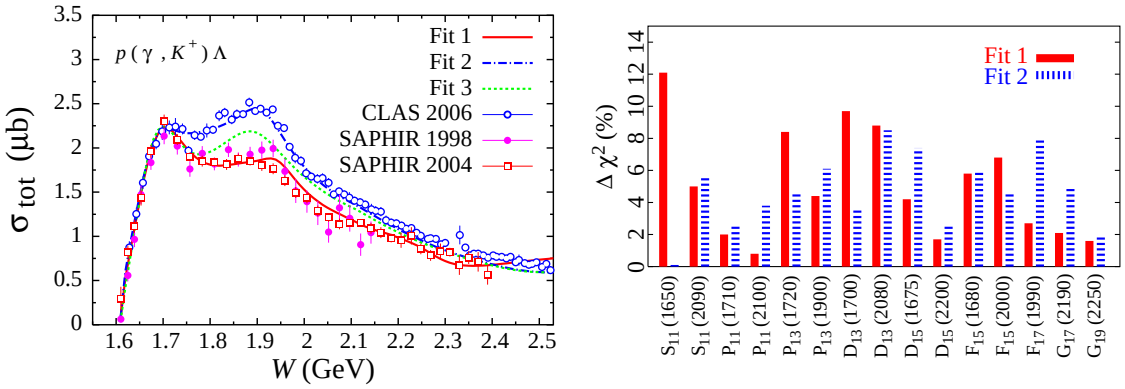

FIGURE 2. **(Left)** Comparison between the calculated total cross sections with experimental data, which clearly shows the discrepancy problem between the CLAS and SAPHIR data [3]. **(Right)** The importance of individual resonances in the multipole models that fit to SAPHIR (Fit 1) and CLAS (Fit 2) data [3]. Note that $\Delta\chi^2 = \left|\chi^2_{\rm All} - \chi^2_{{\rm All}-N^*}\right| / \chi^2_{\rm All} \times 100\,\%$, whereas Fit 3 is obtained by using all data sets.

therefore, could lead to different conclusions on the "missing resonances". This is shown in Fig. 2. Fitting to the SAPHIR data (denoted by Fit 1 in the figure) indicates that the $S_{11}(1650)$, $P_{13}(1720)$, $D_{13}(1700)$, $D_{13}(2080)$, $F_{15}(1680)$, and $F_{15}(2000)$ resonances are required, while fitting to the of CLAS (Fit 2) data leads alternatively to the $P_{13}(1900)$, $D_{13}(2080)$, $D_{15}(1675)$, $F_{15}(1680)$, and $F_{17}(1990)$ resonances. Fitting both data sets simultaneously (Fit 3) yields a compromise result and changes this conclusion which indicates that the corresponding result is neither consistent with Fit 1 nor with Fit 2.

Although yielding different results in most cases (see Fig. 3) both SAPHIR and CLAS data indicate that the second peak in the total cross sections at $W \sim 1900$ MeV, shown in the left panel of Fig. 2, originates from the $D_{13}(2080)$ resonance. By refitting the Kaon-Maid model to the CLAS and SAPHIR data individually, it is shown that the extracted masses of the missing resonance $D_{13}(1895)$ differ only by 11 MeV [12]. The same situation is also found in the multipole model [3]. This is clearly demonstrated in

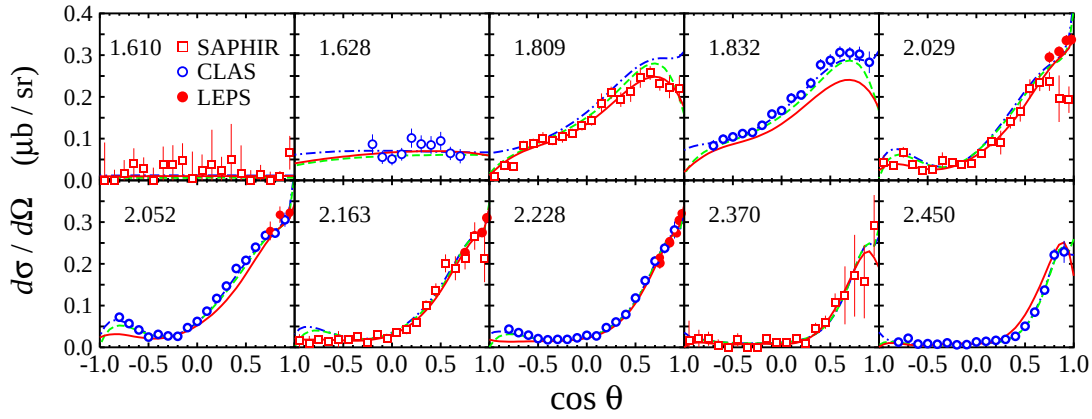

FIGURE 3. Comparison between the calculated differential cross sections obtained from a multipole model [3] with some selected experimental data. Notation for the curves is as in Fig. 2.

TABLE 1. The values of mass (M) and width (Γ) of the missing D_{13} resonance extracted from Kaon-Maid using the three different experimental data [12] and from a multipole model using SAPHIR and CLAS data [3].

	Kaon-Maid			Multipole	
	Original [5]	SAPHIR [8]	CLAS [9]	SAPHIR [8]	CLAS [9]
M (GeV)	1.895 ± 0.004	1.938 ± 0.004	1.927 ± 0.003	1.936 ± 0.010	1.915 ± 0.004
Γ (GeV)	0.372 ± 0.029	0.233 ± 0.008	0.570 ± 0.019	0.301 ± 0.022	0.165 ± 0.008

Table 1. The extracted widths, however, vary from 165 to 570 MeV.

The Gerasimov-Drell-Hearn (GDH) sum rule also provides another tool to investigate the physics difference between the CLAS and SAPHIR data. The sum rule relates the anomalous magnetic moment of the nucleon κ_N to the difference of its polarized total photoabsorption cross sections [14]. Since there has been no available measurement, these cross sections must be predicted from a reliable model which fits all existing unpolarized experimental data. The two models (Fit 1 and Fit 2) described above can be used for this purpose. It is found that the two data sets yield quite different contributions [15]. The predicted contribution of Fit 1 is much closer to that of the Kaon-Maid, indicating the consistency of the new SAPHIR data [8] to the old ones [5]. The model that fits the CLAS differential cross section data (Fit 2) tends to eliminate the contribution of kaon-hyperon final states to the GDH sum rule.

2.2. Influence of the New C_x and C_z Data

Recently, a set of the beam-recoil polarization observables data, C_x and C_z, has been released by the CLAS collaboration [17]. These data indicate that the Λ polarization is predominantly in the direction of the spin of the incoming photon, independent of the c.m. energy or the kaon scattering angle (see Fig. 4). Recent analyses found that these data seems to be difficult to explain. Clearly, it is interesting to include these data in our analysis, as well as to investigate the effects of the data inclusion [15]. After including these data it is found that the total cross sections $\sigma_{\mathrm{TT}'}$ show less structures. This indicates that the CLAS C_x and C_z data select certain resonances as the important ones. To investigate this phenomenon, in Fig. 5 we plot contributions of several important resonances to the total cross section $\sigma_{\mathrm{TT}'}$ before and after the inclusion of the C_x and C_z data [15]. It is obvious from this figure that the inclusion emphasizes the roles of the $S_{11}(1650)$, $P_{11}(1710)$, $P_{13}(1720)$, and $P_{13}(1900)$ resonances, which corroborates the finding of the authors of Ref. [16]

3. ELECTROMAGNETIC PRODUCTIONS OF $K\Sigma$

Photoproductions of $K\Sigma$ are of interest because existing models that can nicely reproduce the $K^+\Sigma^0$ data could overestimate the charged Σ data by almost two orders of magnitude [18]. In these channels the amplitudes F_i, can be expressed in terms of three independent isospin amplitudes, i.e. $A^{(0)}$ for the isoscalar photon, $A^{(1/2)}$ and $A^{(3/2)}$ for

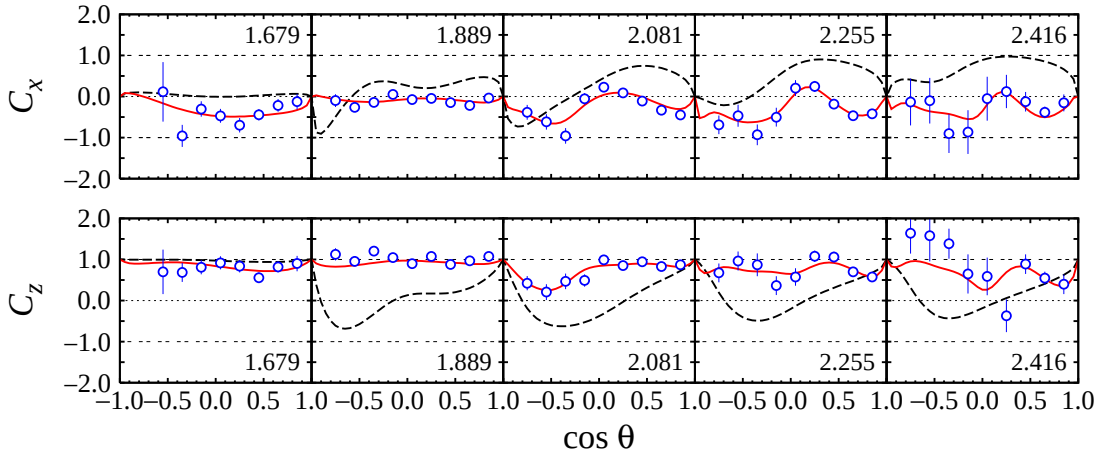

FIGURE 4. Sample of the beam-recoil polarization observables C_x and C_z for the reaction $\vec{\gamma}p \to K^+\vec{\Lambda}$ plotted as a function of the kaon scattering angle. Experimental data are taken from Ref. [17]. The corresponding total c.m. energy W is shown in each panel. Dashed curves show the prediction of Kaon-Maid, solid curves demonstrate the result of the multipole model after including the C_x and C_z data.

the isovector photon with total isospin of the KY system $I = 1/2$ and $I = 3/2$, respectively. For comparison with the results of previous calculations, as well as with the PDG values [20], it is also useful to define the proton ${}_pA^{(1/2)}$ and neutron ${}_nA^{(1/2)}$ helicity photon couplings with total isospin 1/2,

$$ {}_pA^{(1/2)} \;=\; A^{(0)} + \tfrac{1}{3}A^{(1/2)} \;\;, \quad {}_nA^{(1/2)} \;=\; A^{(0)} - \tfrac{1}{3}A^{(1/2)} \;. \tag{5} $$

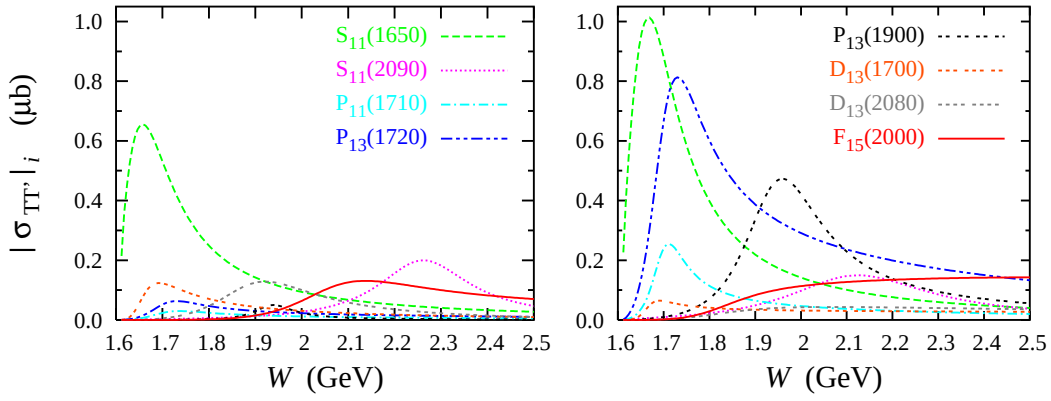

FIGURE 5. The individual contribution of several important resonances to the absolute value of the total cross section $\sigma_{TT'}$ before (left panel) and after (right panel) the inclusion of the beam-recoil polarization observables C_x and C_z. Note that contributions from other resonances are small and, therefore, are not shown in this figure for the sake of clarity.

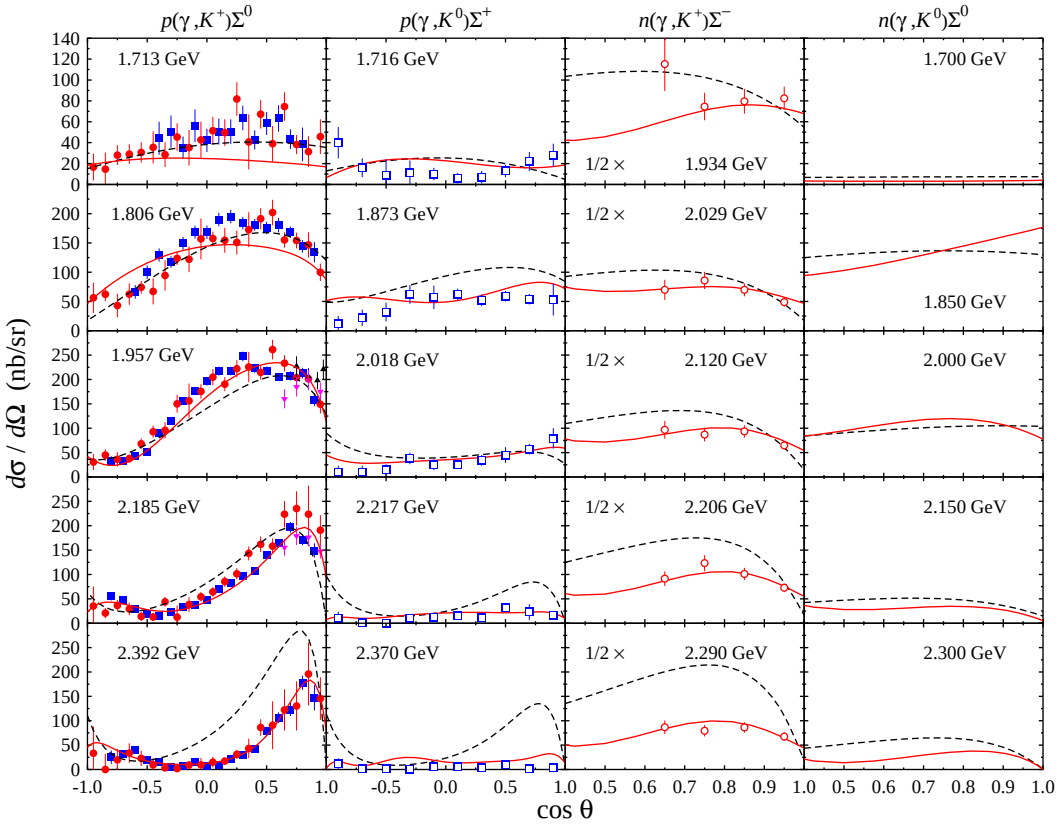

FIGURE 6. Comparison between the calculated differential cross sections from Kaon-Maid (dashed curves) and the present work (solid curves) with selected experimental data for all $K\Sigma$ isospin channels with selected energy bins. Experimental data for the $K^+\Sigma^0$ channel are from SAPHIR (solid circles) [8], CLAS (solid squares) [9], and LEPS (solid triangles) [10, 11]. For the $K^0\Sigma^+$ channel experimental data are taken from SAPHIR (open squares) [19], whereas for the $K^+\Sigma^-$ channel experimental data are from LEPS (open circles) [11]. Note that for the $K^+\Sigma^-$ channel data and curves have been rescaled by a factor of 1/2 in order to fit on the scale.

Using this notation, the CGLN amplitudes for the four physical channels of kaon photoproduction can be written as

$$A(\gamma p \to K^+\Sigma^0) = {}_pA^{(1/2)} + \tfrac{2}{3}A^{(3/2)} , \quad (6)$$

$$A(\gamma n \to K^0\Sigma^0) = -{}_nA^{(1/2)} + \tfrac{2}{3}A^{(3/2)} , \quad (7)$$

$$A(\gamma p \to K^0\Sigma^+) = \sqrt{2}\left[{}_pA^{(1/2)} - \tfrac{1}{3}A^{(3/2)}\right] , \quad (8)$$

$$A(\gamma n \to K^+\Sigma^-) = \sqrt{2}\left[{}_nA^{(1/2)} + \tfrac{1}{3}A^{(3/2)}\right] . \quad (9)$$

All observables are calculated from these amplitudes.

In total we use 2816 data points in our fitting data base. From their types the experimental data used are dominated by the differential cross section data followed by the hyperon recoil polarization ones. From the isospin channel point of view, except for the $K^0\Sigma^0$ channel, all channels have experimental data. Most of the data were collected for

the $K^+\Sigma^0$. Data for the $K^0\Sigma^+$ channel were measured by the SAPHIR collaboration [19] and are given in terms of differential cross section and recoil polarization. For the $K^+\Sigma^-$ channel experimental data were extracted by the LEPS [11] collaboration and are represented by differential cross section and photon asymmetry.

For the background amplitudes we use the similar tree-level Feynman diagrams as in the case of $K\Lambda$. Different from the $K\Lambda$ case, in the $K\Sigma$ case all resonance properties, i.e., the mass, width, branching ratios, as well as the proton and neutron helicity photon couplings are constrained by using the PDG values [20]. In the fitting process we found that the $K^0\Sigma^+$ data require a weighting factor. This is understandable, because the number of data for the $K^0\Sigma^+$ channel is substantially smaller than that for the $K^+\Sigma^0$ channel, and the corresponding error bars are significantly larger. For the fit result shown in Fig. 6 the $K^0\Sigma^+$ channel has been weighted by a factor of 4. Nevertheless, as shown in this figure, compared to the Kaon-Maid prediction the present calculation yields a more satisfactorily result. Predictions for the $K^0\Sigma^0$ channel is also shown in Fig. 6. It is obvious that this channel is very difficult to measure. Our calculation predicts that the corresponding cross section is comparably small as the $K^0\Sigma^+$ cross section. Details of the findings in the $K\Sigma$ channels will be reported elsewhere [21].

ACKNOWLEDGMENTS

The author acknowledges the support from the University of Indonesia.

REFERENCES

1. T. Mart, *Phys. Rev. C* **62**, 038201 (2000); C. Bennhold, H. Haberzettl and T. Mart, arXiv:nucl-th/9909022.
2. T. Mart and C. Bennhold, *Phys. Rev. C* **61**, 012201 (1999).
3. T. Mart and A. Sulaksono, *Phys. Rev. C* **74**, 055203 (2006).
4. H. Haberzettl, C. Bennhold, T. Mart, and T. Feuster, Phys. Rev. C **58**, R40 (1998).
5. M. Q. Tran *et al.*, *Phys. Lett. B* **445**, 20–26 (1998).
6. T. Mart *et al.*, http://www.kph.uni-mainz.de/MAID/kaon/kaonmaid.html.
7. L. Tiator *et al.*, *Eur. Phys. J. A* **19**, 55–60 (2004).
8. K. H. Glander *et al.*, *Eur. Phys. J. A* **19**, 251–273 (2004).
9. R. Bradford *et al.*, *Phys. Rev. C* **73**, 035202 (2006).
10. M. Sumihama *et al.* [LEPS Collaboration], *Phys. Rev. C* **73**, 035214 (2006).
11. H. Kohri *et al.*, *Phys. Rev. Lett.* **97**, 082003 (2006).
12. P. Bydžovský and T. Mart, *Phys. Rev. C* **76**, 065202 (2007).
13. E.L. Crow, F.A. Davis, M.W. Maxfield, *Statistics Manual* (Dover Publication Inc., New York, 1960).
14. S.B. Gerasimov, Sov. J. Nucl. Phys. **2**, 430 (1966); S.D. Drell and A.C. Hearn, Phys. Rev. Lett. **16**, 908 (1966).
15. T. Mart, arXiv:0803.0601 [nucl-th]; *Few Body Syst.* **42**, 125 (2008); *Int. J. Mod. Phys. A* **23**, 599 (2008).
16. A. V. Anisovich, V. Kleber, E. Klempt, V. A. Nikonov, A. V. Sarantsev and U. Thoma, *Eur. Phys. J. A* **34**, 243 (2007).
17. R. Bradford *et al.*, *Phys. Rev. C* **75**, 035205 (2007).
18. T. Mart, C. Bennhold and C. E. Hyde-Wright, *Phys. Rev. C* **51**, 1074 (1995).
19. R. Lawall *et al.*, *Eur. Phys. J. A* **24**, 275 (2005).
20. W.-M. Yao *et al.*, *J. Phys. G* **33**, 1 (2006).
21. T. Mart, in preparation.